

Materials Advances

Accepted Manuscript

This article can be cited before page numbers have been issued, to do this please use: H. Telli, H. Maachou, Y. Zouambia, R. Chebout, H. Derdar, A. Hamitouche, A. Dekir, Y. Larbah, A. Ghawanmeh, E. Brett, A. C. Da Silva and S. Hudson, *Mater. Adv.*, 2026, DOI: 10.1039/D5MA01478F.



This is an Accepted Manuscript, which has been through the Royal Society of Chemistry peer review process and has been accepted for publication.

Accepted Manuscripts are published online shortly after acceptance, before technical editing, formatting and proof reading. Using this free service, authors can make their results available to the community, in citable form, before we publish the edited article. We will replace this Accepted Manuscript with the edited and formatted Advance Article as soon as it is available.

You can find more information about Accepted Manuscripts in the [Information for Authors](#).

Please note that technical editing may introduce minor changes to the text and/or graphics, which may alter content. The journal's standard [Terms & Conditions](#) and the [Ethical guidelines](#) still apply. In no event shall the Royal Society of Chemistry be held responsible for any errors or omissions in this Accepted Manuscript or any consequences arising from the use of any information it contains.

Microwave-Assisted Carboxymethylation of Guar Gum Improves Antioxidant and Antibacterial Activity

H.Telli^{a,b}, H. Maachou^{a,b*}, Y. Zouambia^a, R. Chebout^c, H. Dardar^d, A-E Hamitouche^c, A.Dekir^e, Y. Larbah^f, Abdullah A. Ghawanmeh^g, Elizabeth A. Brett^h, Aruã C. Da Silva^{h*} and Sarah Hudson^{h*}

^a Laboratory of Materials and Environment (LME), Faculty Technology, University of Medea, Medea 26000, Algeria.

^b Departement of Materials science, Faculty of Sciences, University of Medea, Medea 26000, Algeria

^c Scientific and Technical Research Centre in Physico-Chemical Analyses (CRAPC), BP384, Bou-Ismaïl, Tipaza 42004, Algeria.

^d Laboratory of Polymer Chemistry (LCP), Department of Chemistry FSEA, University of Oran 1 Ahmed Ben Bella, Oran 31000, Algeria.

^e Laboratory of Applied Organic Chemistry, Synthesis of Biomolecules and Molecular Modelling Group, Sciences Faculty, Chemistry Department, Badji Mokhtar Annaba University, Box 12, 23000 Annaba, Algeria

^f Materials Physics Department, Nuclear Research Centre of Algiers (CRNA), 02, Boulevard Frantz Fanon, B.P. 399, Algiers (16000), Algeria

^g Department of Pharmacy, Faculty of Pharmacy, Jadara University, P.O. Box 733, Irbid 21110, Jordan.

^h Department of Chemical Sciences, SSPC the Research Ireland Centre for Pharmaceuticals, Bernal Institute, University of Limerick, Limerick V94 T9PX, Ireland

* Correspondence to: hamidamaachou@yahoo.fr, Arua.DaSilva@ul.ie and Sarah.Hudson@ul.ie

Abstract:



1 Guar gum (GG), a naturally occurring polysaccharide derived from *Cyamopsis tetragonoloba*,
2 possesses notable physicochemical and biological properties, but its practical applications are
3 limited by poor solubility, instability, and microbial susceptibility. In this study, microwave-
4 assisted carboxymethylation was employed to efficiently modify GG, yielding carboxymethyl
5 guar gum (CMGG) with a high degree of substitution (DS = 0.64) in 15 minutes. Fourier-
6 transform infrared, proton and carbon-13 nuclear magnetic resonance analyses confirmed
7 functionalization by incorporation of carboxymethyl groups, with a distinct carboxyl peak at
8 1723 cm⁻¹ and a new signal at δ 184.2 ppm corresponding to the carbonyl carbon. Additionally,
9 X-ray diffraction, scanning electron microscopy and thermogravimetric analysis revealed
10 increased crystallinity, morphological alterations including the formation of smaller aggregates
11 and a spongy-like texture, and improved thermal stability. CMGG demonstrated significantly
12 increased antioxidant activity (IC₅₀ = 4.78 ± 0.12 mg/mL) and exhibited pronounced
13 antibacterial effects against *Bacillus cereus*, *Streptococcus thermophilus*, *Staphylococcus*
14 *aureus*, and *Escherichia coli*, outperforming native GG. Molecular docking simulations
15 indicated potential inhibitory interactions between CMGG and dihydropteroate synthase,
16 suggesting a possible mechanism for its antimicrobial activity. Overall, CMGG emerges as
17 multifunctional, biocompatible material with promising potential for biomedical,
18 pharmaceutical, and industrial applications.

19 **Keywords:** Guar gum; Carboxymethylation; Microwave Functionalization; Antioxidant
20 activity; Antibacterial activity; Molecular docking.

21
22
23
24
25

1. Introduction



1 *Cyamopsis tetragonoloba* (guar) is the natural source of GG, a nonionic polysaccharide
2 composed of linear (1→4)-β-D-mannose units randomly substituted with galactose via (1→6)-
3 glycosidic linkages [1]. Due to its renewable origin, biocompatibility, and high viscosity, GG
4 has been widely used in food, pharmaceutical, textile, and petroleum industries [2]. However,
5 its native form exhibits limitations such as excessive swelling, uncontrolled hydration, and
6 microbial instability [3]. To overcome these drawbacks, chemical modifications are commonly
7 applied to tailor the physicochemical and functional characteristics of GG [2]. Among several
8 derivatization techniques, such as sulfation [4], acetylation [5], phosphorylation [6], and
9 selenylation [7], carboxymethylation has gained particular attention for enhancing solubility,
10 viscosity, and microbial resistance through the introduction of carboxymethyl (-CH₂COOH)
11 groups [8,9]. Conventional heating methods to introduce these carboxymethyl groups often
12 require prolonged reaction times and high energy input, leading to heterogeneous reactions and
13 limited scalability [10,11].
14 Microwave-assisted synthesis for the functionalization of polymers has recently emerged as an
15 efficient, eco-friendly alternative to conventional heating methods. This method allows
16 uniform, rapid heating and improved reaction kinetics by coupling electromagnetic radiation
17 with dipolar molecules [11,12]. Guar gum has been successfully functionalized with acrylic
18 acid through microwave-assisted polymerization, enabling higher grafting yields and cleaner
19 reaction profiles than traditional thermal methods [13]. Microwave-assisted techniques have
20 also been applied to carboxymethyl guar gum (functionalized with carboxymethyl groups by
21 conventional heating methods first), resulting in enhanced polyacrylamide chain grafting
22 efficiency and improved functional performance [14]. However, despite these advances,
23 microwave-assisted carboxymethylation of native guar gum itself has not yet been reported.
24 Existing studies focus on microwave-enabled grafting onto pre-modified guar derivatives or
25 other polysaccharides [15], leaving a clear gap regarding the direct introduction of



1 carboxymethyl groups onto the native galactomannan backbone. Beyond structural
2 optimization, carboxymethylation can enhance biological activities such as antioxidant and
3 antimicrobial effects by introducing electron-donating groups that promote free radical
4 scavenging and bacterial membrane disruption [16–21]. However, mechanistic insights into
5 these bioactivities remain limited.

6 In this study, we report a microwave-assisted carboxymethylation strategy for the rapid and
7 energy-efficient derivatization of guar gum. The resulting CMGG exhibits enhanced
8 physicochemical stability, antioxidant, and antimicrobial properties. Furthermore, molecular
9 docking simulations provide insights into the antibacterial mechanism of CMGG at the
10 molecular level. This integrated green synthesis and computational analysis framework
11 highlights CMGG as a promising biopolymer for biomedical and environmental applications.
12

13 **2. Materials and Methods**

14 **2.1 Materials**

15 GG (G4129) with a molecular weight of 220 kDa, monochloroacetic acid (MCA, 402923), and
16 2,2-diphenyl-1-picrylhydrazyl (DPPH, D9132) were obtained from Sigma-Aldrich (Germany).
17 All chemicals utilized were of analytical grade and were used as received without any further
18 purification. Ultrapure water with a resistivity of 18.2 M Ω ·cm was used to prepare all solutions.

19 **2.2 Preparation of CMGG using microwave irradiation**

20 The carboxymethylation of GG was carried out using microwave irradiation based on a
21 previously established method for a different chemical functionalization [13,22], with slight
22 modifications. Briefly, GG (1 g) was dispersed in 2-propanol (15 mL), followed by the addition
23 of 10 M aqueous NaOH (15 mL). The mixture was stirred for 1 hour at 50 °C to allow an initial
24 alkalization. Subsequently, monochloroacetic acid (MCA, 1 g), pre-dissolved in 2-propanol (12
25 mL) and pre-heated at the same temperature (50 °C), was added to the alkaline GG mixture. A



1 range of process parameters were screened in this next microwave assisted step, including oven
2 temperature (35 – 65 °C), time (10 – 20 minutes), monochloroacetic acid amount (0.6 – 1.4 g)
3 and microwave power (100 – 600 W), details on **Table S1**. The following conditions were
4 deemed optimal to achieve microwave-assisted carboxymethylation of GG and the CMGG
5 characterized as described in the following methods was produced using these optimal
6 conditions. Therefore, the reaction mixture was then subjected to microwave irradiation at
7 50 °C for 15 minutes, with 30-second intervals of electromagnetic irradiation at an optimized
8 power of 600 W. After irradiation, the product was cooled to room temperature, washed
9 thoroughly with ethanol, filtered, repeatedly rinsed with deionized water and dried under
10 vacuum at 50 °C for 24 hours. As a control, a separate sample was prepared by treating GG
11 with NaOH solution under the same conditions but without the addition of MCA, to account
12 for any changes due to protonation of intermediate GG species in the absence of MCA. The
13 microwave irradiation protocol is schematically illustrated in **Figure 1**, and the screened
14 reaction conditions, including temperature, reaction time, MCA amount, and irradiation power,
15 are provided in **Supplementary Information**. Biocompatibility tests with human dermal
16 fibroblast cells are also reported (**Supplementary Figure S1**).



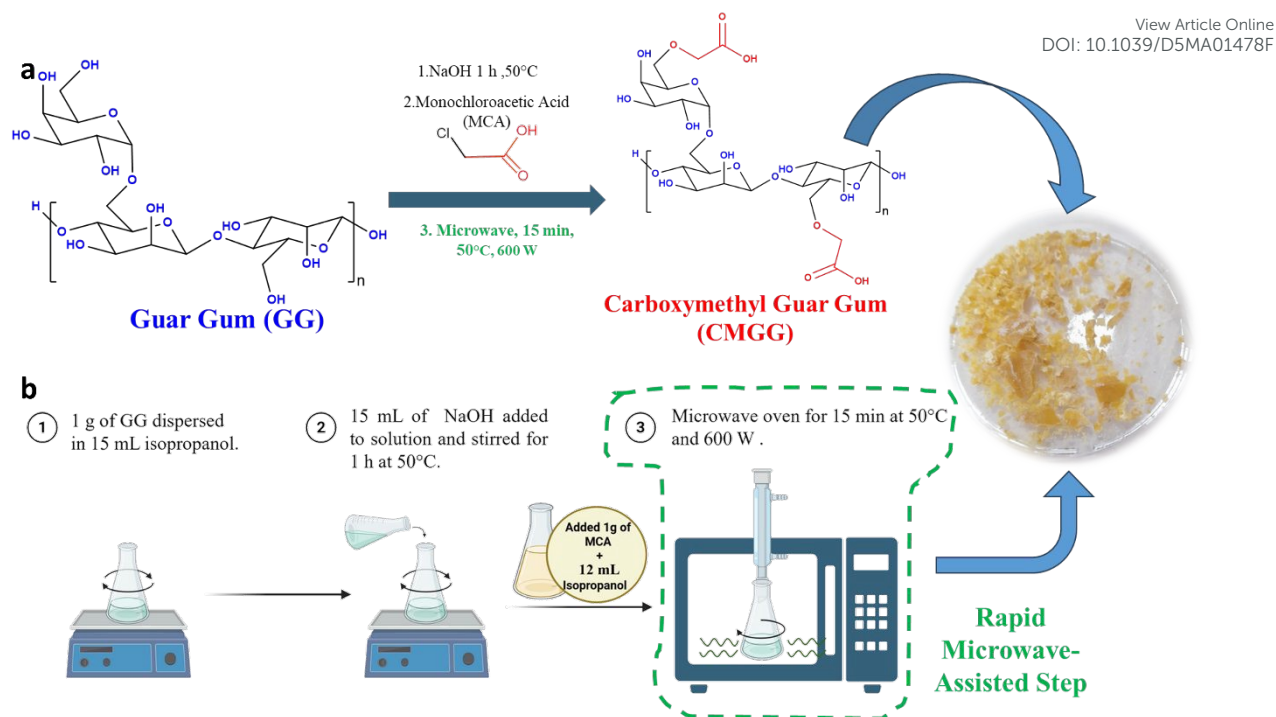


Figure 1. a. Representative chemical reaction with carboxymethyl groups highlighted in red, introduced by monochloroacetic acid (MCA) and details of the optimized microwave-assisted conditions in green. b. Schematic representation of the carboxymethylation process for the natural GG powder. Highlighted in green the rapid microwave-assisted step.

2.3 Characterization techniques

Various characterization techniques were employed to investigate the structural, morphological, thermal, and crystalline properties of GG and CMGG. Scanning electron microscopy (FESEM, JEOL JSM-7200F, USA) was used to analyze surface morphology without gold coating. Proton and carbon nuclear magnetic resonance (^1H and ^{13}C NMR) (Bruker 400 MHz NMR spectrometer) spectra were recorded in deuterated water (D_2O) to confirm structural modifications and determine the degree of substitution after carboxymethylation. Fourier transform infrared spectroscopy (FTIR, Bruker Optics GmbH, Ettlingen, German) was applied in attenuated total reflectance (ATR) mode to identify functional groups and verify chemical changes. Thermogravimetric analysis coupled with differential scanning calorimetry (TGA/DSC using a PerkinElmer STA8000 instrument) was performed to assess thermal stability and degradation behavior, using a heating rate of $10\text{ }^\circ\text{C min}^{-1}$ with samples placed in



1 aluminum pans. Lastly, powder X-ray diffraction (PXRD) was performed using a Rigaku
2 Miniflex II diffractometer equipped with CuK α radiation ($\lambda = 1.5406 \text{ \AA}$) to evaluate the degree
3 of crystallinity of GG and CMGG and assess changes in molecular ordering following chemical
4 modification. Diffraction patterns were collected over a 2θ range of $10\text{--}80^\circ$, using an
5 accelerating voltage of 40 kV and a scanning rate of $10^\circ \text{ min}^{-1}$.

6 *Degree of substitution determination*

7 The DS of CMGG was evaluated using a titrimetric method, as outlined in previously reported
8 protocols [23]. For this, 1 g of CMGG was mixed with 50 mL of methanol, then 5 mL of 0.5 M
9 aqueous solution of nitric acid was added, and the mixture was stirred for 10 min at room
10 temperature. The sample was boiled for 5 min and stirred for 20 min at 300 rpm. After that, the
11 sample was allowed to stand for 30 min. The sample was filtered and washed with ethanol ($3 \times$
12 50 mL) to remove salt and acids. Afterward, the precipitate was washed with methanol (1×50
13 mL), transferred into a beaker, and heated until the alcohol evaporated. The CMGG was dried
14 in a conventional oven at 90°C for 3 h. Then, CMGG was added to 100 mL of distilled water
15 and 25 mL of 0.5 M aqueous solution of NaOH in an Erlenmeyer flask. The solution was heated
16 at 98°C for 1 h. Finally, the heated solution was titrated with 0.3 M HCl using phenolphthalein
17 indicator until neutralization (when the color of the solution changed from magenta to
18 transparent). The same procedure was carried out for a blank solution (0.5 M aqueous solution
19 of NaOH without CMGG). The carboxymethyl group (-COOH content) and the DS were
20 calculated as follows:

$$21 \quad n_{\text{COOH}} = C_{\text{NaOH}} \times V_{\text{NaOH}} - C_{\text{HCl}} \times V_{\text{HCl}} \quad (1)$$

$$22 \quad DS = \frac{162 \times n_{\text{COOH}}}{m - 58 \times n_{\text{COOH}}} \quad (2)$$

23 Where n_{COOH} is the number of moles of COOH groups in the sample, C_{NaOH} and C_{HCl} are the
24 molar concentrations of standard NaOH and HCl solutions, respectively, V_{NaOH} is the volume
25 of NaOH, and V_{HCl} is the volume of HCl used for the titration of the excess of NaOH, DS is the



1 degree of substitution, 162 is the molecular weight of anhydrous glucose unit ($\text{g}\cdot\text{mol}^{-1}$), 58 is
 2 the molecular weight of the carboxymethyl ($-\text{CH}_2\text{COO}^-$) group that replaces the hydroxyl ($-$
 3 OH) group ($\text{g}\cdot\text{mol}^{-1}$) in the GG polymer, and m is the amount of CMGG used for the test (g).
 4 Each titration was repeated at least three times to confirm reproducibility.

6 *DPPH• Free Radical Scavenging investigation*

7 The antioxidant activity of CMGG and GG was assessed using the DPPH (2,2-diphenyl-1-
 8 picrylhydrazyl) free radical scavenging assay, following the protocol described by Moussa *et*
 9 *al.* [24]. Ethanolic suspensions/solutions of GG and CMGG were prepared at various
 10 concentrations ranging from 0.2 to 200 mg/mL. GG exhibited limited solubility under these
 11 conditions. Each solution was mixed with a DPPH solution at a final concentration of 0.023
 12 mg/mL in ethanol. The mixtures were incubated at 25°C in the dark for 30 min to allow the
 13 reaction to proceed without interference from light. The percentage of DPPH• radical
 14 scavenging was obtained by measuring the absorbance at 517 nm using a UV-Vis
 15 spectrophotometer. The scavenging activity percentage was calculated using equation 3 (A_{control}
 16 = absorbance of the DPPH solution without the sample and A_{sample} = absorbance of the DPPH
 17 solution with the sample):

$$18 \quad \text{Radical Scavenging Activity (\%)} = \frac{A_{\text{control}} - A_{\text{sample}}}{A_{\text{control}}} \times 100 \quad (3)$$

20 *Antibacterial Activity*

21 The antibacterial properties of native GG and CMGG were evaluated against several microbial
 22 strains [25]: *Bacillus cereus* (gram positive, American Type Culture Collection (ATCC 14579),
 23 *Streptococcus thermophilus* (gram positive, ATCC 33023), *Staphylococcus aureus* (gram
 24 positive, ATCC 6538), and *Escherichia coli* (gram negative, ATCC 8739). Briefly, the



1 antibacterial activity of the samples was evaluated using a disc diffusion method based on the
2 principles of the standard antibiogram. Sterile Whatman paper discs (6 mm diameter) were
3 impregnated with 2 μL of each test solution (100 mg/mL in DMSO) and placed onto the surface
4 of agar plates previously inoculated with 100 μL of microbial suspension. The turbidity of the
5 bacterial suspensions was adjusted to 10^8 CFU/mL.

6 After placement of the discs using sterile forceps, the agar plates were kept at room temperature
7 for 1 hour to allow diffusion of the samples, followed by incubation at 37 °C for 24 hours.
8 Antimicrobial activity was assessed by measuring the diameter of the inhibition zones formed
9 around the discs. Larger inhibition zones (diameter) indicate greater antimicrobial
10 effectiveness. The statistical analysis was made using two-ways analysis of variance (ANOVA)
11 using OriginLab software. Statistical significance is indicated as follows: $p \leq 0.05$ (*), $p \leq 0.01$
12 (**), and $p \leq 0.001$ (***), based on Tukey's test.

13 *Molecular docking study*

14 To investigate the binding interactions of GG and CMGG within the DHPS pocket, molecular
15 docking simulations were conducted using the Schrödinger Suite. For representing the GG, the
16 (1,4)- β -D-mannose unit bound to 1,6-galactose unit was used. For the CMGG, the same
17 structure was used with carboxymethyl groups at the C6 of mannose and galactose, as shown
18 in the monomer structure of **Figure 1**. The structural data of DHPS was obtained from the
19 RCSB Protein Data Bank (<http://www.pdb.org>) under the PDB ID 3TZF [26]. This enzyme was
20 chosen as the docking target, and it was optimized through energy minimization using the
21 Protein Preparation Wizard in the Schrödinger Suite [27]. The co-crystallized ligand
22 (sulfamethoxazole) and the monomers of GG and CMGG were prepared using LigPrep [28],
23 ensuring appropriate protonation states, correct atom types, the addition of hydrogen atoms and
24 the assignment of bond orders to refine their molecular structures for docking. The docking grid
25 was generated using the Receptor Grid Generation protocol in Maestro [29], with the centroid



1 of the bound ligand set as the grid center. Default parameters were applied for grid generation.
2 The flexible docking simulations were carried out in single precision (SP) mode [30], enabling
3 accurate ligand-protein interaction predictions while considering molecular flexibility.
4

5 3. Results and Discussion

6 3.1 Carboxymethylation of Guar Gum

7 Carboxymethylation of guar gum (GG) has been well reported in the literature but only by
8 conventional heating methods[8,10,11]. Here, from the range of process parameters screened
9 (**Table S1**), the highest degree of carboxymethylation of one gramme of GG via a microwave-
10 assisted method was obtained when one gramme of monochloroacetic acid was used with
11 microwaves of 600 W at a temperature of 50°C for 15 minutes.

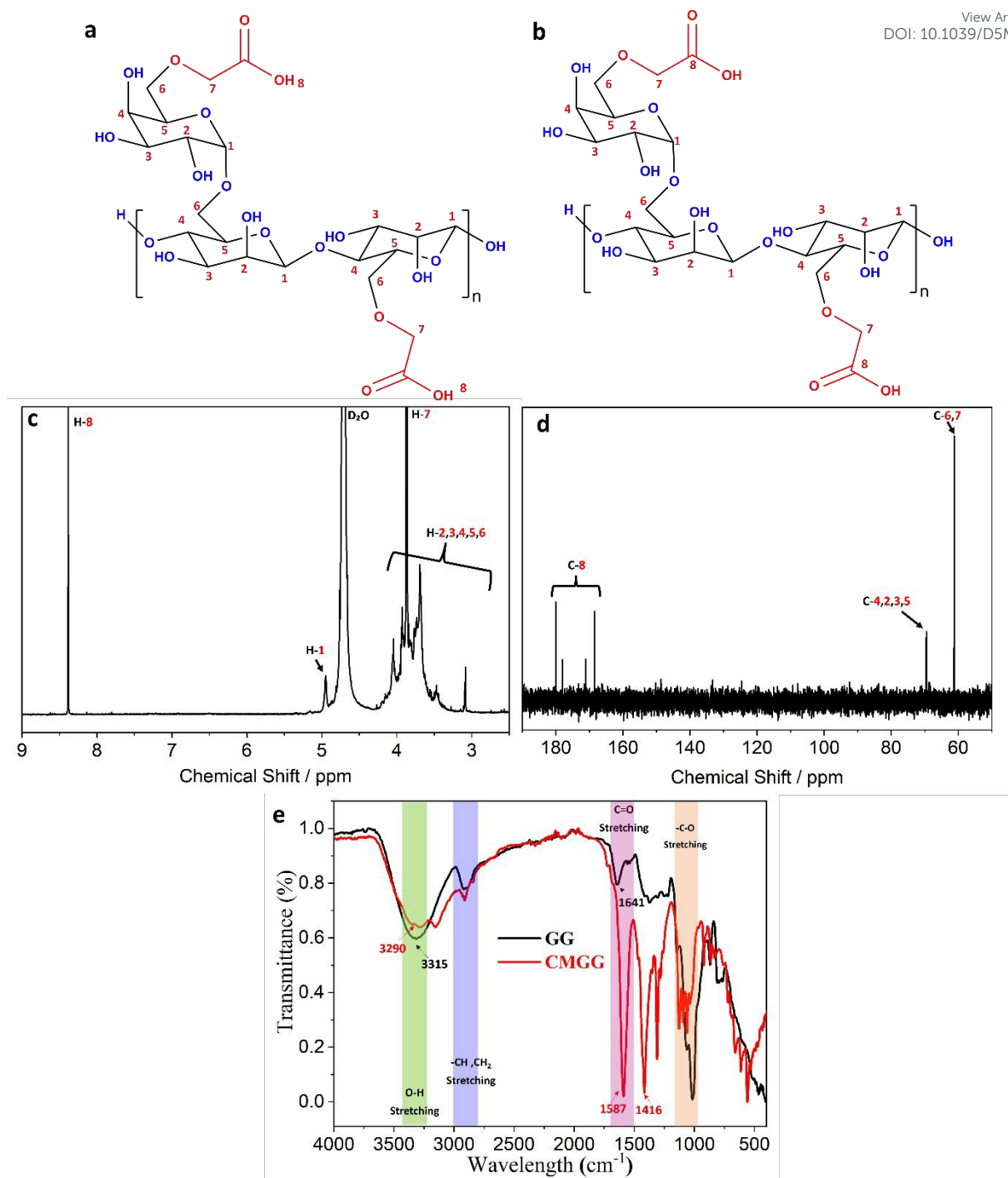
12 Using this method, ¹H NMR and ¹³C NMR analysis confirmed the successful
13 carboxymethylation of CMGG (**Figure 2** and **S2**). The ¹H NMR spectrum of CMGG (**Figure**
14 **2a**) displays characteristic up field signals in the range of δ 3.0 – 5.0 ppm, which correspond to
15 the sugar protons of the polysaccharide backbone. These protons are associated with hydroxyl
16 and ring hydrogen atoms in the GG structure (**Figure 2c**) [10,31,32]. Additionally, the strong
17 signal at δ 3.86 and 8.38 ppm in the CMGG spectrum is attributed to the methylene protons (-
18 CH₂-) and hydroxyl group of the carboxylic groups (-COOH), respectively. The peak at δ 8.38
19 ppm is difficult to corroborate with previous literature, as most studies report only the δ 3.0–
20 5.0 ppm region [10,31,32].

21 The ¹³C spectrum of CMGG (**Figure 2b**) shows signals at δ 179.9 –168.3 ppm corresponding
22 to the carbonyl carbon of the carboxylic groups (-COOH) introduced through the
23 carboxymethylation process. Additionally, carbon signals in the CMGG ¹³C spectrum appear
24 in the range of δ 61.1 – 69.5 ppm, corresponding to the carbons C2–C6 of the polysaccharide



1 backbone. The shift in proton signals and the appearance of the carboxylic carbon signal is
2 consistent with successful carboxymethylation of the GG [33,34].
3 A distinct absorption peak observed at 1587 cm^{-1} and 1416 cm^{-1} in the FTIR spectrum of CMGG
4 (**Figure 2e**) corresponds to the stretching vibrations of the $>\text{C}=\text{O}$ bonds in the carboxylic acid
5 groups, confirming the successful chemical modification of GG by the introduction of
6 carboxymethyl functionalities. Notably, in the comparative spectra of GG and CMGG,
7 differences in characteristic bands are observed in the region between 1725 and 1000 cm^{-1} ,
8 suggesting structural changes associated with carboxymethylation. A detailed assignment of
9 the characteristic absorption bands for the individual spectra of GG and CMGG is provided in
10 supplementary information (**Figure S3**), which further supports the incorporation of
11 carboxymethyl groups. Thus, the NMR and FTIR spectroscopic analyses provided strong
12 evidence for the successful carboxymethylation of guar gum, aligned with previous reports in
13 the literature [10,11,35]



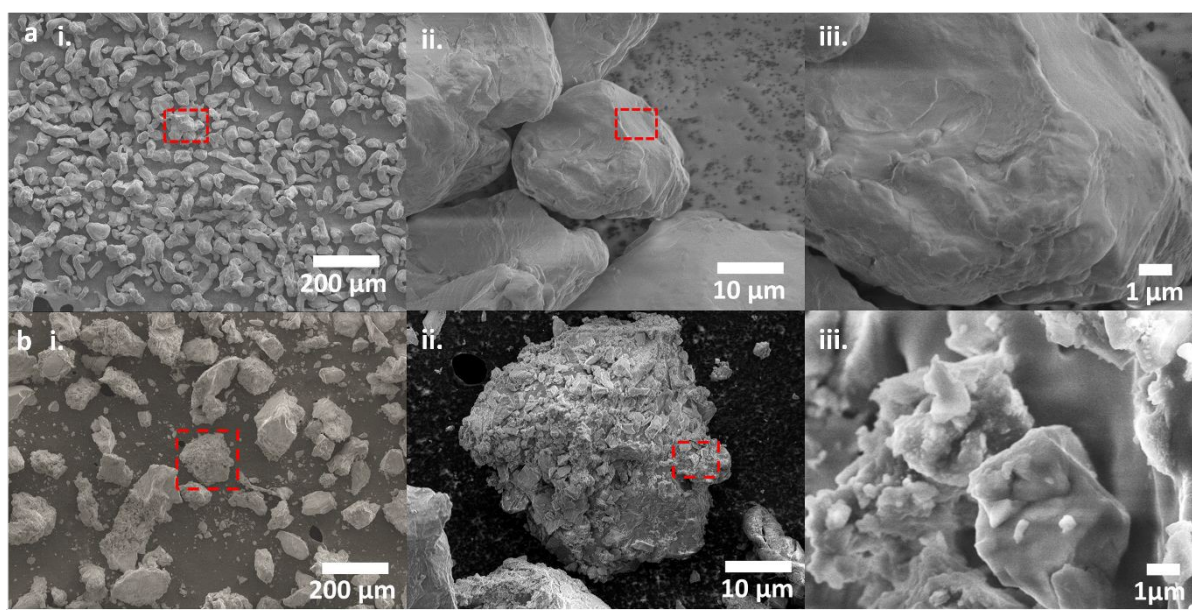
View Article Online
DOI: 10.1039/D5MA01478F

1
2 **Figure 2.** (a, c) ^1H NMR and (b, d) ^{13}C NMR spectra of CMGG with the ^1H and ^{13}C assignments, respectively,
3 and (e) FTIR comparative spectra of unmodified GG (black line) and CMGG (red line), highlighting the structural
4 changes upon modification.

5
6 The carboxymethylation of guar gum using this microwave assisted functionalization method
7 also caused macroscopic morphological changes to the polymer, including the formation of



1 smaller aggregates and a spongy-like texture compared to its original smooth, uniform particles.
 2 **Figure 3.** The CMGG particles exhibit agglomeration and increased porosity, compared to GG.
 3 These structural changes suggest enhanced surface activity, which may improve the material's
 4 reactivity and functionality, particularly for applications involving adsorption or molecular
 5 interactions. Similar morphological trends have been observed in other chemically modified
 6 polysaccharides [36]. This sponge-like texture was absent in GG when it was exposed to the
 7 process conditions for carboxymethylation in the absence of MCA (**Figure S4**), confirming that
 8 the structural changes were due to the carboxymethylation reaction. The increased porosity and
 9 agglomeration observed in CMGG may contribute to improved solubility, surface area, and
 10 reactivity, further supporting its potential applications in biomedicine, food packaging, and
 11 water treatment.

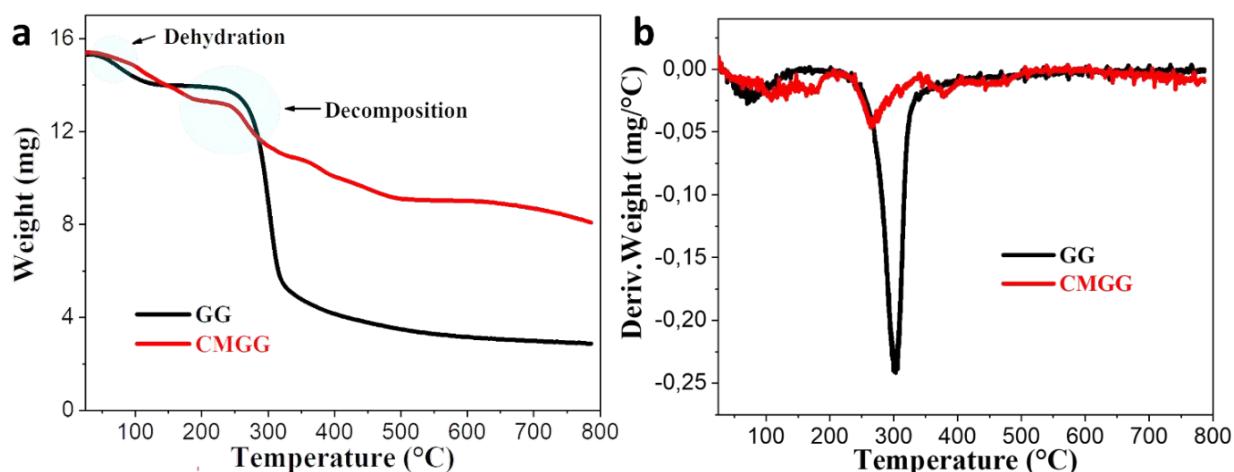


12
 13 **Figure 3.** SEM images of (a, top) GG and (b, bottom) CMGG, respectively. The red dashed squares represent the
 14 region where higher magnification was executed. Scale bars are 100 μm (i, left), 10 μm (ii, center) and 1 μm (iii,
 15 right), respectively.

16
 17 GG undergoes two major weight loss events upon heating: an initial loss around 100°C due to
 18 the evaporation of adsorbed water [37] and a second step at 264°C, attributed to polymer



1 degradation, **Figure 4**. The char residue at 600°C is approximately 5%, likely due to the
 2 presence of inorganic fillers or stabilizers [38]. For CMGG, a more gradual weight loss with
 3 increasing temperature is observed, leading to a final loss in weight of 47% between room
 4 temperature and 600°C, accompanied by a higher char residue compared to GG, **Figure 4a**.
 5 This gradual loss in mass suggests improved thermal stability due to the incorporation of
 6 carboxymethyl groups, which enhance crosslinking and reduce the formation of volatile
 7 degradation products. The presence of residual inorganic salts from the carboxymethylation
 8 reaction may also contribute to this stability [38,39]. The derivative thermogravimetric (DTG)
 9 (**Figure 4b**) shows that GG exhibits a degradation peak at 303°C, consistent with previous
 10 findings [40] while CMGG displays a smaller peak at 265°C, possibly due to the presence of
 11 uncross-linked chains. Tamba *et al.* reported a similar degradation temperature at 241 °C (57%
 12 mass loss) for CMGG (261 kDa), functionalized via a conventional heating method (50 °C for
 13 4h) and 262 °C (70% mass loss) for native GG (220 kDa).[41]

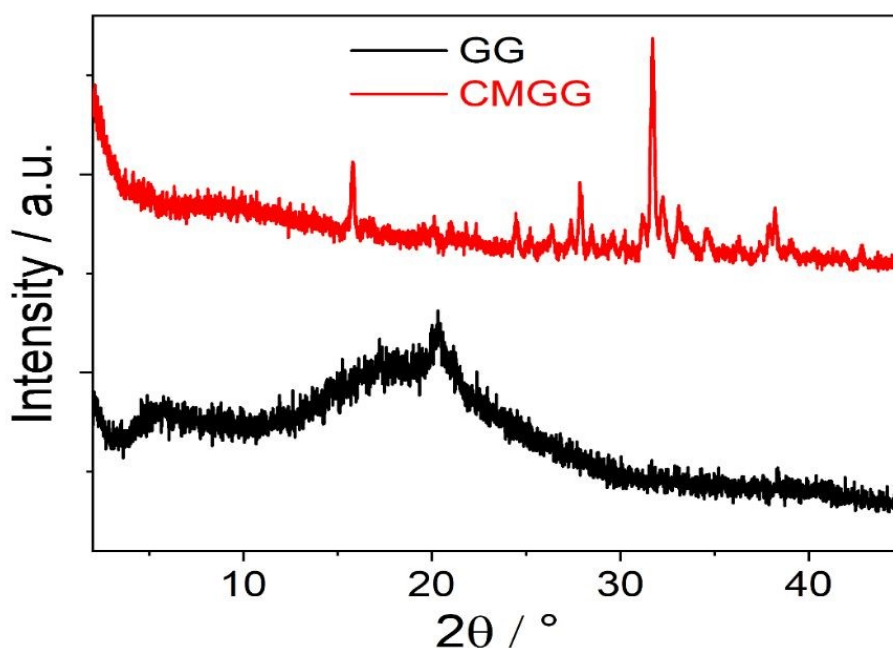


14
 15 **Figure 4.** Thermograms TGA (a) and DTG (b) profiles of GG (black line) and CMGG (red line).
 16

17 Powder X-ray diffraction analysis of both unmodified GG and CMGG, indicated structural
 18 changes induced by the chemical modification, **Figure 5**. The diffractogram of unmodified GG
 19 (black line) displays a predominantly amorphous nature, characterized by a broad diffraction



1 peak centered at a 2θ angle of $\sim 20^\circ$. In contrast, the diffractogram of CMGG (red line) reveals
2 a significant transformation in its structural profile, transitioning from the predominantly
3 amorphous nature of unmodified GG to a semi-crystalline state. This transition is evidenced by
4 the emergence of sharper and more intense diffraction peaks, indicating enhanced molecular
5 ordering due to the carboxymethylation process. This was also evidenced from the observation
6 of distinct melting peaks in DSC thermograms for CMGG which were absent for GG, **Figure**
7 **S5**. The introduction of carboxymethyl groups likely disrupts the random coil conformations of
8 the GG backbone, facilitating partial alignment of polymer chains and the formation of more
9 organized crystalline regions. Additionally, these modifications enhance intra- and
10 intermolecular interactions, including hydrogen bonding and electrostatic forces, which further
11 stabilize the crystalline domains.



12 **Figure 5.** PXR D Diffractograms of unmodified GG (black line) and CMGG (red line).

13
14
15 Microwave-assisted carboxymethylation of GG at 600 W in 15 minutes (optimized condition,
16 **Table S1**) achieved a DS of 0.64, significantly improving reaction efficiency over conventional



1 heating at 50 °C, which required 2-4 hours for similar results, **Table 1** [42]. In the microwave-
 2 assisted esterification of guar gum, Nazir *et al.* reported degradation of GG only at more than
 3 15 minutes of reaction time at a power of 1000 W.[43] Given that the microwave exposure time
 4 in our experimental conditions was only up to 15 minutes, no polymer degradation is expected.

5
 6 **Table 1.** Degree of carboxymethylation of CMGG compared with values reported.

Reference	Polymer	DS	Carboxymethylation method	Time
<i>Gong et al.</i> [44]	Guar gum	0.6	Conventional method 60°C	10 h
<i>G. Dodi et al</i> [42]	Guar gum	0.64	Conventional method 50°C	4 h
<i>S. Pal</i> [8]	Guar Gum	0.4-0.7	Conventional method 50°C	2 h
<i>Present work</i>	Guar gum	0.64	Microwave-assisted 50°C	15 min

7
 8 The superior performance of microwave-assisted synthesis is due to its unique heating
 9 mechanism, where electromagnetic waves interact directly with polar molecules, ensuring rapid
 10 and uniform temperature increase. This process overcomes diffusion limitations, improving
 11 reaction kinetics and molecular transport [45]. Additionally, microwave irradiation enhances
 12 selectivity and efficiency by (i) generating localized heating, reducing side reactions; (ii)
 13 increasing reagent solubility and accessibility; and (iii) rapidly activating molecular bonds,
 14 accelerating the reaction. The optimized power level of 600 W (**Table S1**) ensures efficient
 15 energy transfer while minimizing polysaccharide degradation, making the process reproducible
 16 and scalable for industrial applications. Beyond efficiency, microwave-assisted synthesis aligns
 17 with green chemistry principles, reducing energy consumption and reaction times. These
 18 findings underscore its potential as a sustainable and high-performance approach for
 19 polysaccharide modification, with broad applications in materials science.

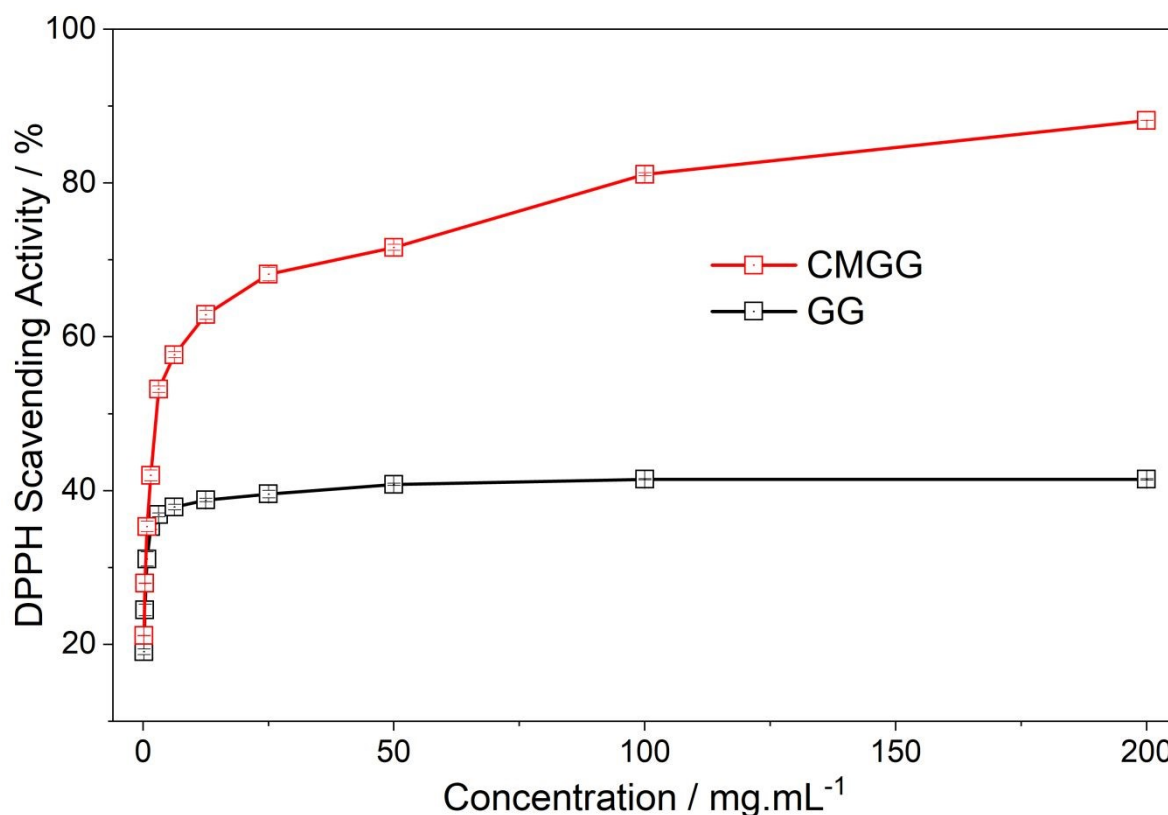


3.2 Antioxidant Activity of CMGG and GG

1 CMGG, with a DS of 0.64, exhibited high antioxidant activity, achieving approximately 80%
2 DPPH radical inhibition at a concentration of 200 mg/mL, with an IC_{50} of ~ 4.78 mg/mL (**Figure**
3 **6**). This activity was found to be concentration-dependent, with higher concentrations leading
4 to greater radical scavenging. In comparison, an IC_{50} value could not be achieved against DPPH
5 radicals at a DPPH concentration of 0.023 mg/mL with unmodified GG, even with up to 200
6 mg of GG added per mL, likely due to the poor solubility of GG. This suggests that the
7 introduction of carboxylic groups through modification enhances the antioxidant capacity of
8 GG [46], and is likely due to a combination of optimized DS, enhanced water solubility, and
9 the electron-donating ability of carboxymethyl groups. Previous studies have shown that
10 increasing the concentration of CMGG from 3 to 8 wt% leads to a marked increase in viscosity
11 and the emergence of non-Newtonian, pseudoplastic behavior. [11,32] This behavior is
12 commonly attributed to enhanced polymer–solvent interactions and improved chain
13 disentanglement resulting from carboxymethyl substitution. Pal et al. (2009) compared the
14 rheological properties of native guar gum (GG) and CMGG prepared via a conventional
15 carboxymethylation method (DS ≈ 0.6). Both polymers were evaluated at a low concentration
16 of 0.5 wt%. However, at this concentration, the complete solubilization of native GG is
17 questionable, which complicates a direct comparison of intrinsic rheological properties. Despite
18 this limitation, Pal et al. reported a similar non-Newtonian behavior for both systems, with
19 CMGG exhibiting a slightly higher viscosity.[8]
20
21 This DPPH scavenging activity assay primarily reflects the ability of a compound to donate
22 electrons or hydrogen atoms to neutralize the stable DPPH radical, providing an initial
23 indication of antioxidant potential at the chemical level. The enhanced scavenging activity
24 observed for CMGG therefore suggests that the carboxymethylation of guar gum introduces
25 structural features that improve its radical quenching capability in solution. However, the



1 potential demonstrated by DPPH assay do not fully represent antioxidant activity in cellular
 2 system.



3
 4 **Figure 6.** Evaluation of antioxidant activity of GG (black) and CMGG (red) using a DPPH solution at a final
 5 concentration of 0.023 mg/mL in ethanol.
 6

7 The effect of chemical substitution on antioxidant performance has been extensively studied in
 8 GG derivatives. Phosphorylated GG, with DS values of 0.37, 0.43 and 0.52, showed improved
 9 DPPH scavenging activity, with IC₅₀ values of 1.74, 1.45, and 1.32 mg/mL, respectively [47].
 10 Sulfated GG variants such as SGG_{cata3} and SGG_{cata7} achieved high inhibition levels of 80.32%
 11 and 79.35% at 5 mg/mL. Among these, SGG_{cata3}—featuring a higher DS and lower molecular
 12 weight—demonstrated the most potent activity [48]. Additionally, sulfated GG has also been
 13 reported to exhibit strong antioxidant potential due to the incorporation of sulfate groups, which
 14 increase negative charge density and facilitate radical stabilization. In another study, sulfated
 15 GG showed approximately 75% scavenging at 1 mg/mL against DPPH radicals [49].



1 Furthermore, phosphorylated GG achieved around 78% scavenging with an IC₅₀ of ~5.5 µg/mL,
2 attributed to the phosphate groups enhancing hydrogen atom transfer mechanisms [50,51].
3 Bioactive films produced by CMGG have demonstrated over 95% DPPH scavenging at
4 concentrations above 500 µg/mL [52], highlighting the significant enhancement of antioxidant
5 functionality through carboxymethylation. The present study indicates that the IC₅₀ of 4.78
6 mg/mL achieved with CMGG is consistent with the range of antioxidant activities reported for
7 GG-based derivatives in the literature[53].
8 Outside of GG-based systems, the influence of DS on antioxidant activity has been similarly
9 observed. Carboxymethylated polysaccharides from *Amana edulis* with DS values ranging from
10 0.605 to 0.783 exhibited high in vitro antioxidant activity (77.3–99.9%), while native
11 polysaccharides showed much lower activity (20–75%) [54]. Carboxymethylated cashew gum
12 also displayed strong DPPH scavenging with an IC₅₀ of 0.43 mg/mL [55]. Similarly,
13 carboxymethylated *Sargassum fusiforme* polysaccharides showed improved antioxidant
14 performance, increasing from 60.05% in the native form to 66.6% upon modification [56].
15 Phosphorylated pumpkin polysaccharides with DS values ranging from 0.33 to 0.52
16 demonstrated 55% to 70% radical scavenging activity, confirming the trend of DS-dependent
17 antioxidant efficiency in non-GG polysaccharides as well [57].
18 Comparing the antioxidant performances of various modified polysaccharides, CMGG stands
19 out by offering a strong balance of solubility and functional group reactivity. The
20 carboxymethylation process introduces carboxymethyl groups (-CH₂COOH), which not only
21 enhance solubility but also provide hydrogen atoms that facilitate electron donation and radical
22 stabilization [56], confirming preliminary antioxidant potential of the modified polymer.

23

24 3.7 Antibacterial Activity



1 In this work, CMGG exhibited significantly larger inhibition zones, compared to native GG (p
2 < 0.05), for all four tested bacterial strains (*Bacillus cereus*, *Streptococcus thermophilus*,
3 *Staphylococcus aureus*, and *Escherichia coli*), indicating an enhanced antimicrobial effect,
4 **Figure 7.** For *Bacillus cereus*, the zone expanded from 6.2 ± 0.8 mm (GG) to 15.2 ± 0.2 mm
5 (CMGG); for *Streptococcus thermophilus*, from 10.4 ± 0.6 mm to 15.1 ± 0.3 mm; for
6 *Staphylococcus aureus*, from 11.1 ± 1.0 mm to 13.6 ± 0.4 mm; and for *Escherichia coli*, from
7 11.5 ± 0.5 mm to 13.1 ± 0.2 mm, upon treatment with GG or CMGG respectively.

8 This enhancement suggests that the carboxymethylation of guar gum introduces functional
9 groups that improve its interaction with bacterial cell membranes, thereby increasing its
10 antibacterial efficacy. The modification likely enhances the solubility, charge distribution, and
11 molecular interactions of the polysaccharide, all of which can contribute to the disruption of
12 microbial growth. Representative images of the inhibition zones from the disc diffusion assays
13 are provided in **Figure S6**.

14 Carboxymethylation has been widely reported to enhance the antimicrobial properties of
15 various polysaccharides by introducing functional groups that improve solubility, charge
16 distribution, and molecular interactions with bacterial membranes. For instance, carboxymethyl
17 β -glucans exhibited significant antibacterial activity against *Staphylococcus aureus*, with
18 maximum inhibition zones reaching 19.37 ± 0.45 mm [58]. Similarly, carboxymethylated
19 derivatives of degraded *Sargassum fusiforme* polysaccharide (DPSF) showed inhibition zones
20 of 11.10 ± 0.04 mm and 14.68 ± 0.05 mm against *Escherichia coli* and *Staphylococcus aureus*,
21 respectively. In contrast, neither the native polysaccharide nor its degraded form exhibited any
22 noticeable antibacterial activity, highlighting the critical role of carboxymethylation in its
23 activity [59]. Liu *et al.* also reported that chloroacetic acid-modified *Catathelasma ventricosum*
24 polysaccharides displayed elevated antibacterial activity against *E. coli*, *Salmonella*
25 *typhimurium*, *S. aureus*, and *Bacillus subtilis* [60]. Furthermore, carboxymethylated kappa-



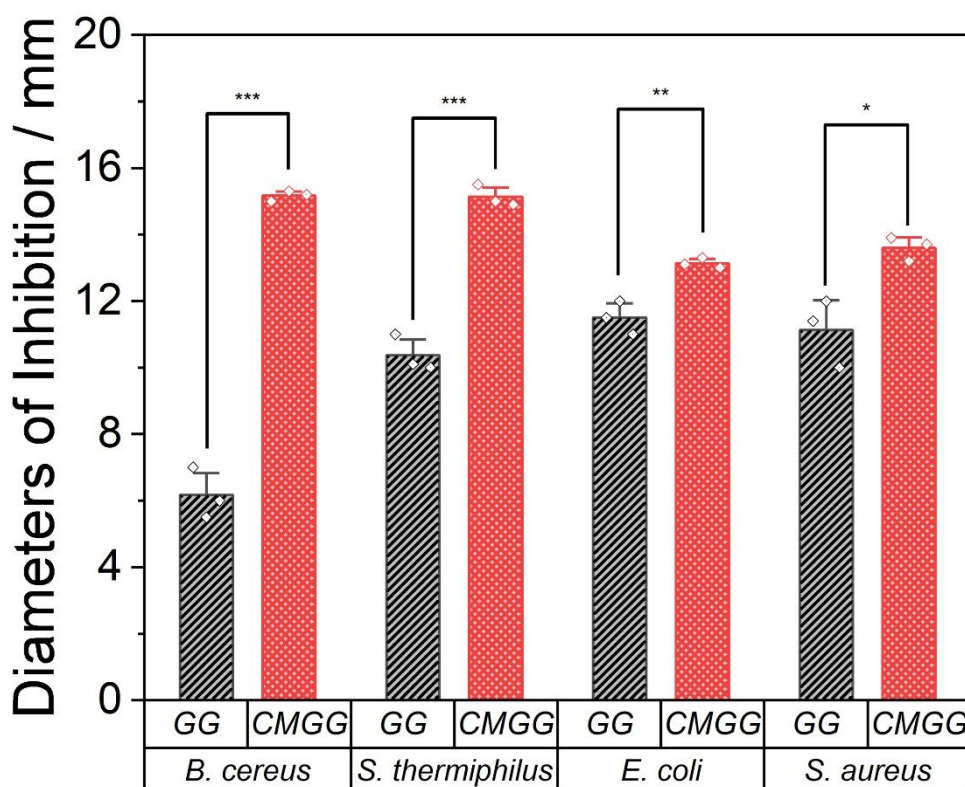
1 carrageenan with degrees of substitution ranging from 0.8 to 1.6 demonstrated markedly
2 increased antimicrobial efficacy against *S. aureus*, *B. cereus*, and *E. coli* when compared to the
3 native kappa-carrageenan [61].

4 CMGG exhibited markedly higher antibacterial activity against the Gram-positive strains *B.*
5 *cereus* and *S. thermophilus*, with inhibition levels significantly greater than those observed for
6 the Gram-negative species ($p \leq 0.001$). This enhanced susceptibility of Gram-positive bacteria
7 is commonly attributed to their cell-wall architecture: they lack an outer membrane and possess
8 a more permeable peptidoglycan layer, allowing the negatively charged carboxylate groups of
9 CMGG to interact more effectively with positively charged components of the cell wall. Such
10 interactions are likely to destabilize the membrane and promote leakage of intracellular
11 materials.

12 In contrast, *E. coli* and *S. aureus* showed lower sensitivity to CMGG, with statistically
13 significant but smaller reductions in bacterial growth ($p \leq 0.01$ for *E. coli* and $p \leq 0.05$ for *S.*
14 *aureus*). For Gram-negative species, the outer membrane acts as an additional barrier that
15 restricts penetration of high-molecular-weight or polyanionic compounds such as CMGG. The
16 reduced activity against *S. aureus*, compared with the other Gram-positive strains, may further
17 be explained by its dense peptidoglycan layer, characteristic teichoic acid composition, and its
18 ability to form biofilms, all of which can hinder polymer–cell wall interactions.[62]

19 Overall, these results indicate that the antibacterial performance of CMGG is strongly
20 influenced by both its carboxymethyl substitution and the structural features of the target
21 microorganisms, which together dictate cell-wall accessibility and susceptibility.





1
2 **Figure 7.** Antibacterial activity of GG and CMGG against *Bacillus cereus*, *Streptococcus thermophilus*,
3 *Escherichia coli* and *Staphylococcus aureus*, respectively. Statistical significance is indicated as follows: $p \leq 0.05$
4 (*), $p \leq 0.01$ (**), and $p \leq 0.001$ (***), based on Tukey's test.

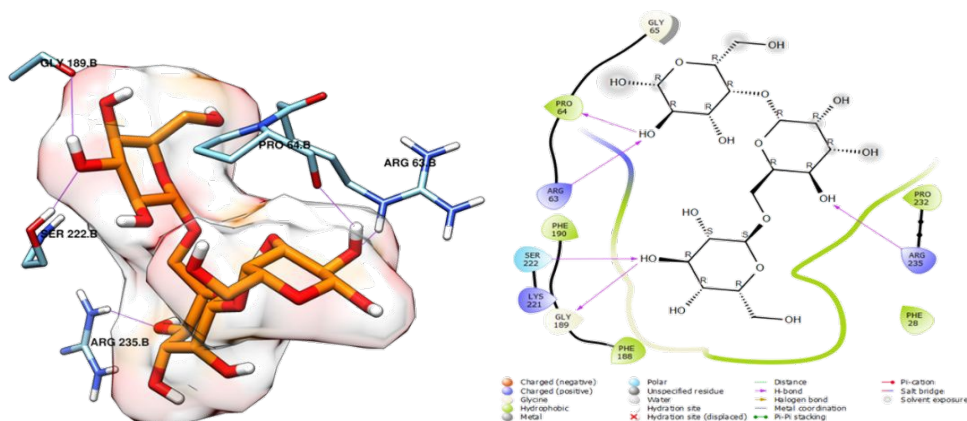
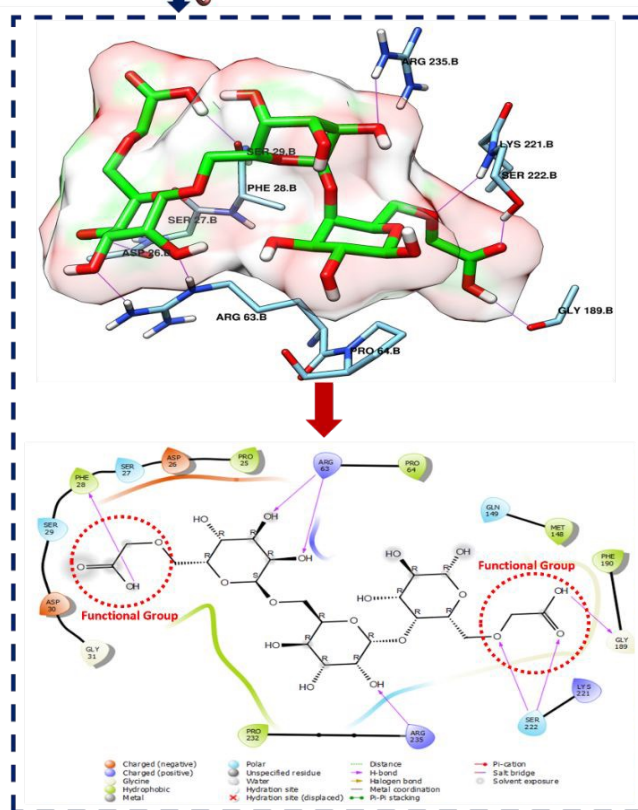
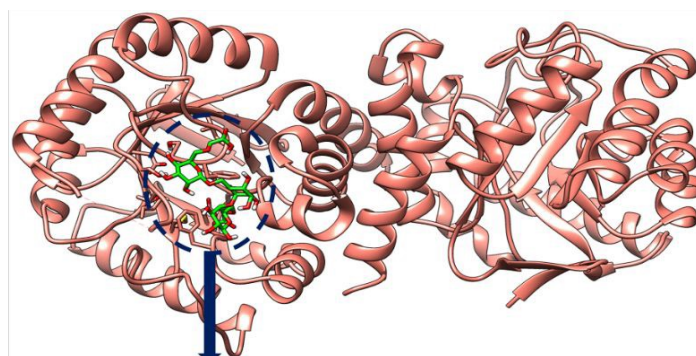
5
6 DHPS is an example of an enzyme that is targeted by existing antimicrobial agents, such as
7 sulfonamides, trimethoprim and aminosalicylic [63,64]. When DHPS is inhibited, the
8 synthesis of folic acid in bacteria is inhibited, causing death [65]. To investigate the feasibility
9 of DHPS inhibition as the antibacterial mechanism of action of GG and CMGG, molecular
10 docking simulations targeting DHPS, utilizing both the GG unit and the carboxymethyl
11 modified version CMGG, were conducted. The goal was to compare their binding affinities and
12 interactions with the enzyme and hypothesise the mechanism behind the observed antibacterial
13 activity. Our docking protocol was validated by redocking the co-crystallized ligand
14 (sulfamethoxazole), achieving an RMSD value of less than 1 Å, as shown in **Figure S7**.
15 Although docking a single disaccharide unit inherently oversimplifies the complexity of a
16 polymeric system, it represents a well-established strategy in the literature for gaining initial



1 insights into polysaccharide–protein interactions.[66] Additionally, the higher binding affinity
2 demonstrated for the modified guar gum unit suggests DHPS might play a role in the observed
3 antibacterial activity.

4 The molecular docking results reveal a significant improvement in the binding affinity of the
5 modified polymer unit (CMGG) compared to the original unmodified unit (GG), with docking
6 scores of -8.125 kcal/mol and -4.652 kcal/mol, respectively. For reference, the docking score is
7 -6.100 kcal/mol for the co-crystallized ligand typically designed to interact with the specific
8 enzyme site. This difference can be attributed to the presence of the carboxyl group, which
9 introduces additional interactions with the bacterial DHPS target. Specifically, seven hydrogen
10 bonds were formed between the hydroxyl (OH) groups and the residues SER222, GLY189,
11 ARG63, ARG235, and PHE28, three of which were created through the added carboxyl
12 functionality, as illustrated in **Figure 8**.





1
2 **Figure 8.** Binding interaction of CMGG (top) and GG (bottom) within the active site of DHPS, highlighting the
3 calculated structure and interactions with groups in the active site (dark blue dashed square).
4



1 In contrast, the unmodified unit (GG) exhibits weaker affinity and limited interactions, forming
2 only five hydrogen bonds with the residues PRO64, ARG63, SER222, GLY189, and ARG23,
3 suggesting poorer recognition by the active site of the DHPS target, **Figure 8**.

4 The enhanced molecular interactions due to carboxyl functionalization can be explained by the
5 ability of this group to form strong hydrogen bonds and interact with key residues of the
6 bacterial DHPS receptor. These results suggest that chemical modification of the guar gum
7 polysaccharide could enhance its antibacterial activity by promoting better binding to the active
8 site of the target, and that DHPS inhibition is a feasible mechanism of action for the observed
9 CMGG antibacterial activity (**Figure 7**). The overall biocompatibility of CMGG, which is like
10 GG, showed no toxicity towards human dermal fibroblasts (**Figure S1**) combined with its'
11 enhanced antioxidant and antibacterial activity, indicates its' potential for use in biomedical
12 applications.

14 4. Conclusion

15 This study confirmed our hypothesis that a microwave-assisted method can be used to achieve
16 carboxymethylation of GG quickly and with a high degree of substitution. The resulting
17 carboxymethylated polymer, CMGG, exhibited significantly enhanced antioxidant and
18 antibacterial properties due to improvements in the polymer solubility, charge distribution, and
19 functional group accessibility. The microwave-assisted synthesis route enabled rapid and
20 efficient carboxymethylation, achieving an optimal DS of 0.64, while drastically reducing
21 reaction time compared to conventional heating methods. Structural and thermal
22 characterization revealed that the modified biopolymer CMGG exhibits higher crystallinity,
23 distinct morphological changes, and improved thermal stability, confirming its enhanced
24 structural robustness. Critically, CMGG demonstrated superior bioactivity compared to native
25 GG, with a notable antioxidant capacity ($IC_{50} = 4.78 \pm 0.12$ mg/mL) and strong antibacterial



1 effects against both Gram-positive (*Bacillus cereus*, *Streptococcus thermophilus*,
2 *Staphylococcus aureus*) and Gram-negative (*Escherichia coli*) strains. These findings support
3 our hypothesis that carboxymethylation enhances bioactivity by facilitating electrostatic
4 interactions with microbial membranes and improving functional group availability.
5 Furthermore, molecular docking simulations suggested that CMGG may inhibit DHPS, a key
6 enzyme in microbial folate biosynthesis, providing a plausible mechanism for its antimicrobial
7 action. Collectively, these results demonstrate that microwave-assisted carboxymethylation is
8 a promising strategy to functionalize GG for biomedical and industrial applications.

11 **CRedit authorship contribution statement**

12 **Hayet Telli:** Conceptualization, methodology, formal analysis, visualization, and original draft
13 preparation. **Hamida Maachou:** Conceptualization, methodology, visualization Supervision,
14 reviewing, and editing. **Yamina Zouambia:** Conceptualization, methodology, visualization
15 Co-Supervision, reviewing and editing. **Redouane Chebout:** Conceptualization, visualization.
16 **Hodhaifa Derdar:** Conceptualization, visualization. **Adh'ya-eddine Hamitouche:**
17 Conceptualization, visualization. **Ali Dekir:** Conceptualization, Data curation, visualization.
18 **Youssef Larbah:** Conceptualization, visualization. **Abdullah A. Ghawanmeh:**
19 Conceptualization, visualization. **Eliza E. Brett:** Conceptualization, methodology,
20 visualization. **Aruã C. Da Silva:** Conceptualization, Supervision, methodology, visualization,
21 formal analysis, Data curation, original draft preparation, critical revision, substantial
22 rewriting, and final editing. **Sarah Hudson:** Conceptualization, methodology, visualization,
23 Supervision, reviewing, and editing.

24 **Acknowledgements**



1 The authors express their sincere thanks to the Government of Ireland (under the Disruptive
2 Technologies Innovation Fund Grant No. DT/2023/445), SSPC the Research Ireland Centre for
3 Pharmaceuticals (under grant no. 12/RC/2275_P2), Department of Chemical Sciences, Bernal
4 Institute, University of Limerick, Ireland; Scientific and Technical Research Centre in Physico-
5 Chemical Analyses (CRAPC), Algeria for some of the physico-chemical analyses and the
6 General Directorate of Scientific Research and Technological Development (DGRSDT),
7 Algeria for funding the physico-chemical analysis via the Ibtikar platform.

8 9 **Data availability**

10 The data given in the current research are available upon request from the corresponding author.

11 12 **References**

- 13 [1] D. Mudgil, S. Barak, B.S. Khatkar, Guar gum: processing, properties and food
14 applications—A Review, *J. Food Sci. Technol.* 51 (2014) 409–418.
15 <https://doi.org/10.1007/s13197-011-0522-x>.
- 16 [2] M. Sharahi, S.H. Bahrami, A. Karimi, A comprehensive review on guar gum and its
17 modified biopolymers: Their potential applications in tissue engineering, *Carbohydr.*
18 *Polym.* 347 (2025) 122739. <https://doi.org/10.1016/j.carbpol.2024.122739>.
- 19 [3] M. Dehghani Soltani, H. Meftahizadeh, M. Barani, A. Rahdar, S.M. Hosseinikhah, M.
20 Hatami, M. Ghorbanpour, Guar (*Cyamopsis tetragonoloba* L.) plant gum: From
21 biological applications to advanced nanomedicine, *Int. J. Biol. Macromol.* 193 (2021)
22 1972–1985. <https://doi.org/10.1016/j.ijbiomac.2021.11.028>.
- 23 [4] J. Wang, B. Zhao, X. Wang, J. Yao, J. Zhang, Structure and antioxidant activities of
24 sulfated guar gum: Homogeneous reaction using DMAP/DCC catalyst, *Int. J. Biol.*
25 *Macromol.* 50 (2012) 1201–1206. <https://doi.org/10.1016/j.ijbiomac.2012.03.009>.



- 1 [5] T.-Y. Huang, F.-L. Yang, H.-W. Chiu, H.-C. Chao, Y.-J. Yang, J.-H. Sheu, K.-F. Hua, S.-H. Wu, An Immunological Polysaccharide from *Tremella fuciformis*: Essential Role
2 of Acetylation in Immunomodulation, *Int. J. Mol. Sci.* 23 (2022) 10392.
3 <https://doi.org/10.3390/ijms231810392>.
- 4 [6] S. Yu, M. Duan, R. Zeng, F. Chen, W. Zhong, J. Sun, J. Xu, D. Li, Y. Zheng, X. Liu, J.
5 Pang, C. Wu, Preparation, characterization and biological activity of phosphorylated
6 surface deacetylated chitin nanofibers, *Int. J. Biol. Macromol.* 233 (2023) 123492.
7 <https://doi.org/10.1016/j.ijbiomac.2023.123492>.
- 8 [7] J. Zhang, Y. Li, Y. Li, Y. Li, X. Gong, L. Zhou, J. Xu, Y. Guo, Structure, selenization
9 modification, and antitumor activity of a glucomannan from *Platycodon grandiflorum*,
10 *Int. J. Biol. Macromol.* 220 (2022) 1345–1355.
11 <https://doi.org/10.1016/j.ijbiomac.2022.09.029>.
- 12 [8] S. Pal, Carboxymethyl guar: Its synthesis and macromolecular characterization, *J.*
13 *Appl. Polym. Sci.* 111 (2009) 2630–2636. <https://doi.org/10.1002/app.29338>.
- 14 [9] V.P. Chakka, T. Zhou, Carboxymethylation of polysaccharides: Synthesis and
15 bioactivities, *Int. J. Biol. Macromol.* 165 (2020) 2425–2431.
16 <https://doi.org/10.1016/j.ijbiomac.2020.10.178>.
- 17 [10] G., H.D., and P.M.I. Dodi, Carboxymethylation of guar gum: synthesis and
18 characterization., *Cellulose Chemistry and Technology* 3 (2011) 171–176.
- 19 [11] H. Gong, M. Liu, J. Chen, F. Han, C. Gao, B. Zhang, Synthesis and characterization of
20 carboxymethyl guar gum and rheological properties of its solutions, *Carbohydr. Polym.*
21 88 (2012) 1015–1022. <https://doi.org/10.1016/j.carbpol.2012.01.057>.
- 22 [12] S. Li, H. Ma, P. Ouyang, Y. Li, Y. Duan, Y. Zhou, W.-J. Ong, F. Dong, Advanced
23 microwave synthesis strategies for innovative photocatalyst design, *Green Energy &*
24 *Environment* 10 (2025) 1597–1623. <https://doi.org/10.1016/j.gee.2024.11.005>.
- 25



- 1 [13] S.B. Shruthi, C. Bhat, S.P. Bhaskar, G. Preethi, R.R.N. Sailaja, Microwave Assisted
2 Synthesis of Guar Gum Grafted Acrylic Acid/Nanoclay Superabsorbent Composites
3 and Its Use in Crystal Violet Dye Absorption, *Green and Sustainable Chemistry* 06
4 (2016) 11–25. <https://doi.org/10.4236/gsc.2016.61002>.
- 5 [14] S. Pal, S. Ghorai, M.K. Dash, S. Ghosh, G. Udayabhanu, Flocculation properties of
6 polyacrylamide grafted carboxymethyl guar gum (CMG-g-PAM) synthesised by
7 conventional and microwave assisted method, *J. Hazard. Mater.* 192 (2011) 1580–
8 1588. <https://doi.org/10.1016/j.jhazmat.2011.06.083>.
- 9 [15] V. Thakur, S. Dhiman, T.G. Singh, R. Bhatia, A. Awasthi, The Cutting Edge Quest:
10 Epic Saga of Carboxymethyl Guar Gum in Drug Delivery and Roads Ahead, *Polym.*
11 *Adv. Technol.* 36 (2025). <https://doi.org/10.1002/pat.70119>.
- 12 [16] L. Wang, Y. Zhao, Y. Wang, F. Zhang, Y. Wei, N. Li, Y. Xu, Preparation, stability,
13 and antibacterial activity of carboxymethylated *Anemarrhena asphodeloides*
14 polysaccharide-chitosan nanoparticles loaded curcumin, *Int. J. Biol. Macromol.* 264
15 (2024) 130787. <https://doi.org/10.1016/j.ijbiomac.2024.130787>.
- 16 [17] M.Q. Guo, X. Hu, C. Wang, L. Ai, Polysaccharides: Structure and Solubility, in:
17 Solubility of Polysaccharides, InTech, 2017. <https://doi.org/10.5772/intechopen.71570>.
- 18 [18] S.-Y. Xu, X. Huang, K.-L. Cheong, Recent Advances in Marine Algae
19 Polysaccharides: Isolation, Structure, and Activities, *Mar. Drugs* 15 (2017) 388.
20 <https://doi.org/10.3390/md15120388>.
- 21 [19] L.C.G.F. Palhares, J.A. London, A.M. Kozlowski, E. Esposito, S.F. Chavante, M. Ni,
22 E.A. Yates, Chemical Modification of Glycosaminoglycan Polysaccharides, *Molecules*
23 26 (2021) 5211. <https://doi.org/10.3390/molecules26175211>.



- 1 [20] X. Chen, M. Shen, Q. Yu, Y. Chen, J. Xie, Recent advance in chemistry modified methods of natural polysaccharides and their applications, Trends Food Sci. Technol. 2
3 144 (2024) 104317. <https://doi.org/10.1016/j.tifs.2023.104317>. View Article Online
DOI: 10.1039/D5MA01478F
- 4 [21] M.M. Ahmad, Recent trends in chemical modification and antioxidant activities of
5 plants-based polysaccharides: A review, Carbohydrate Polymer Technologies and
6 Applications 2 (2021) 100045. <https://doi.org/10.1016/j.carpta.2021.100045>.
- 7 [22] S. Pal, S. Ghorai, M.K. Dash, S. Ghosh, G. Udayabhanu, Flocculation properties of
8 polyacrylamide grafted carboxymethyl guar gum (CMG-g-PAM) synthesised by
9 conventional and microwave assisted method, J. Hazard. Mater. 192 (2011) 1580–
10 1588. <https://doi.org/10.1016/j.jhazmat.2011.06.083>.
- 11 [23] Ž. Stojanović, K. Jeremić, S. Jovanović, M.D. Lechner, A comparison of some
12 methods for the determination of the degree of substitution of carboxymethyl starch,
13 Starch/Staerke 57 (2005) 79–83. <https://doi.org/10.1002/star.200400342>.
- 14 [24] H. Moussa, F. Dahmoune, M. Hentabli, H. Remini, L. Mouni, Optimization of
15 ultrasound-assisted extraction of phenolic-saponin content from *Carthamus caeruleus*
16 L. rhizome and predictive model based on support vector regression optimized by
17 dragonfly algorithm, Chemometrics and Intelligent Laboratory Systems 222 (2022).
18 <https://doi.org/10.1016/j.chemolab.2022.104493>.
- 19 [25] P.J. Manna, T. Mitra, N. Pramanik, V. Kavitha, A. Gnanamani, P.P. Kundu, Potential
20 use of curcumin loaded carboxymethylated guar gum grafted gelatin film for
21 biomedical applications, Int. J. Biol. Macromol. 75 (2015) 437–446.
22 <https://doi.org/10.1016/j.ijbiomac.2015.01.047>.
- 23 [26] J.J. Liu, R. Horst, V. Katritch, R.C. Stevens, K. Wüthrich, Biased signaling pathways
24 in β 2-adrenergic receptor characterized by 19F-NMR, Science (1979). 335 (2012)
25 1106–1110. <https://doi.org/10.1126/science.1215802>.



- 1 [27] L. Schrödinger, Maestro , version 10.6, (2016).
- 2 [28] L. Schrödinger, LigPrep, Version 3.8 , (2016).
- 3 [29] L. Schrödinger, Schrödinger Suite 2016 Update 2, (2016).
- 4 [30] L. Schrödinger, Glide, version 7.1, (2016).
- 5 [31] G. Dodi, A. Pala, E. Barbu, D. Peptanariu, D. Hritcu, M.I. Popa, B.I. Tamba,
6 Carboxymethyl guar gum nanoparticles for drug delivery applications: Preparation and
7 preliminary in-vitro investigations, *Materials Science and Engineering: C* 63 (2016)
8 628–636. <https://doi.org/10.1016/j.msec.2016.03.032>.
- 9 [32] J. Gao, B.P. Grady, Reaction Kinetics and Subsequent Rheology of Carboxymethyl
10 Guar Gum Produced from Guar Splits, *Ind. Eng. Chem. Res.* 57 (2018) 7345–7354.
11 <https://doi.org/10.1021/acs.iecr.8b00782>.
- 12 [33] C. Tranquilan-Aranilla, N. Nagasawa, A. Bayquen, A. Dela Rosa, Synthesis and
13 characterization of carboxymethyl derivatives of kappa-carrageenan, *Carbohydr.*
14 *Polym.* 87 (2012) 1810–1816. <https://doi.org/10.1016/j.carbpol.2011.10.009>.
- 15 [34] T. Muschin, T. Yoshida, Structural analysis of galactomannans by NMR spectroscopy,
16 *Carbohydr. Polym.* 87 (2012) 1893–1898.
17 <https://doi.org/10.1016/j.carbpol.2011.08.059>.
- 18 [35] P. Orsu, S. Matta, Fabrication and characterization of carboxymethyl guar gum
19 nanocomposite for application of wound healing, *Int. J. Biol. Macromol.* 164 (2020)
20 2267–2276. <https://doi.org/10.1016/j.ijbiomac.2020.07.322>.
- 21 [36] D. Sardar, M. Sengupta, A. Bordoloi, M.A. Ahmed, S.K. Neogi, S. Bandyopadhyay, R.
22 Jain, C.S. Gopinath, T. Bala, Multiple functionalities of Ni nanoparticles embedded in
23 carboxymethyl guar gum polymer: catalytic activity and superparamagnetism, *Appl.*
24 *Surf. Sci.* 405 (2017) 231–239. <https://doi.org/10.1016/j.apsusc.2017.01.229>.



- 1 [37] G. Dodi, A. Pala, E. Barbu, D. Peptanariu, D. Hritcu, M.I. Popa, B.I. Tamba, View Article Online
DOI: 10.1039/D5MA01478F
2 Carboxymethyl guar gum nanoparticles for drug delivery applications: Preparation and
3 preliminary in-vitro investigations, *Materials Science and Engineering C* 63 (2016)
4 628–636. <https://doi.org/10.1016/j.msec.2016.03.032>.
- 5 [38] J. Patel, B. Maji, N.S.H.N. Moorthy, S. Maiti, Xanthan gum derivatives: Review of
6 synthesis, properties and diverse applications, *RSC Adv.* 10 (2020) 27103–27136.
7 <https://doi.org/10.1039/d0ra04366d>.
- 8 [39] M. Baghel, K. Sakure, T.K. Giri, S. Maiti, K.T. Nakhate, S. Ojha, C. Sharma, Y.
9 Agrawal, S. Goyal, H. Badwaik, Carboxymethylated Gums and Derivatization:
10 Strategies and Significance in Drug Delivery and Tissue Engineering, *Pharmaceuticals*
11 16 (2023). <https://doi.org/10.3390/ph16050776>.
- 12 [40] J.H. Trivedi, M.D. Thaker, H.C. Trivedi, Photo-induced graft copolymerization of
13 acrylonitrile onto sodium salt of partially carboxymethylated guar gum, *J. Appl. Polym.
14 Sci.* 132 (2015). <https://doi.org/10.1002/app.41371>.
- 15 [41] G. Dodi, A. Pala, E. Barbu, D. Peptanariu, D. Hritcu, M.I. Popa, B.I. Tamba,
16 Carboxymethyl guar gum nanoparticles for drug delivery applications: Preparation and
17 preliminary in-vitro investigations, *Materials Science and Engineering: C* 63 (2016)
18 628–636. <https://doi.org/10.1016/j.msec.2016.03.032>.
- 19 [42] G. Dodi, D. Hritcu, M.I. Popa, CARBOXYMETHYLATION OF GUAR GUM:
20 SYNTHESIS AND CHARACTERIZATION, 2011.
- 21 [43] M. Iqbal, D. Iqbal, E. Hussain, G. Soomro, H. Rizvi, A. Nazir, Microwave assisted
22 green synthesis of guar gum esters with enhanced physico-chemical properties, *Scientia
23 Iranica* 0 (2018) 0–0. <https://doi.org/10.24200/sci.2018.50112.1515>.



- 1 [44] H. Gong, M. Liu, J. Chen, F. Han, C. Gao, B. Zhang, Synthesis and characterization of
2 carboxymethyl guar gum and rheological properties of its solutions, *Carbohydr. Polym.*
3 88 (2012) 1015–1022. <https://doi.org/10.1016/j.carbpol.2012.01.057>.
4 [45] J. Jacob, L.H.L. Chia, F.Y.C. Boey, Review Thermal and non-thermal interaction of
5 microwave radiation with materials, 1995.
6 [46] M. Sharahi, S.H. Bahrami, A. Karimi, A comprehensive review on guar gum and its
7 modified biopolymers: Their potential applications in tissue engineering, *Carbohydr.*
8 *Polym.* 347 (2025). <https://doi.org/10.1016/j.carbpol.2024.122739>.
9 [47] J. Wang, T. Yang, J. Tian, T. Zeng, X. Wang, J. Yao, J. Zhang, Z. Lei, Synthesis and
10 characterization of phosphorylated galactomannan: The effect of DS on solution
11 conformation and antioxidant activities, *Carbohydr. Polym.* 113 (2014) 325–335.
12 <https://doi.org/10.1016/j.carbpol.2014.07.028>.
13 [48] J. Wang, B. Zhao, X. Wang, J. Yao, J. Zhang, Structure and antioxidant activities of
14 sulfated guar gum: Homogeneous reaction using DMAP/DCC catalyst, *Int. J. Biol.*
15 *Macromol.* 50 (2012) 1201–1206. <https://doi.org/10.1016/j.ijbiomac.2012.03.009>.
16 [49] J. Wang, B. Zhao, X. Wang, J. Yao, J. Zhang, Structure and antioxidant activities of
17 sulfated guar gum: Homogeneous reaction using DMAP/DCC catalyst, *Int. J. Biol.*
18 *Macromol.* 50 (2012) 1201–1206. <https://doi.org/10.1016/j.ijbiomac.2012.03.009>.
19 [50] S. Niu, J. Wang, B. Zhao, M. Zhao, M. Nie, X. Wang, J. Yao, J. Zhang, Regioselective
20 synthesis and antioxidant activities of phosphorylated guar gum, *Int. J. Biol.*
21 *Macromol.* 62 (2013) 741–747. <https://doi.org/10.1016/j.ijbiomac.2013.09.047>.
22 [51] J. Wang, T. Yang, J. Tian, T. Zeng, X. Wang, J. Yao, J. Zhang, Z. Lei, Synthesis and
23 characterization of phosphorylated galactomannan: The effect of DS on solution
24 conformation and antioxidant activities, *Carbohydr. Polym.* 113 (2014) 325–335.
25 <https://doi.org/10.1016/j.carbpol.2014.07.028>.



- 1 [52] Tanvi Singh, M. Tanwar, R.K. Gupta, Carboxymethyl Guar Gum-Based Bioactive and
2 Biodegradable Film for Food Packaging, *Polymer Science - Series A* (2024).
3 <https://doi.org/10.1134/S0965545X24600388>.
4 [53] T. Zivari-Ghader, M.R. Rashidi, M. Mehrali, Biological macromolecule-based
5 hydrogels with antibacterial and antioxidant activities for wound dressing: A review,
6 *Int. J. Biol. Macromol.* 279 (2024). <https://doi.org/10.1016/j.ijbiomac.2024.134578>.
7 [54] Y.Y. Cao, Y.H. Ji, A.M. Liao, J.H. Huang, K. Thakur, X.L. Li, F. Hu, J.G. Zhang, Z.J.
8 Wei, Effects of sulfated, phosphorylated and carboxymethylated modifications on the
9 antioxidant activities in-vitro of polysaccharides sequentially extracted from *Amana*
10 *edulis*, *Int. J. Biol. Macromol.* 146 (2020) 887–896.
11 <https://doi.org/10.1016/j.ijbiomac.2019.09.211>.
12 [55] Y. Liu, G. Huang, The antioxidant activities of carboxymethylated cushaw
13 polysaccharide, *Int. J. Biol. Macromol.* 121 (2019) 666–670.
14 <https://doi.org/10.1016/j.ijbiomac.2018.10.108>.
15 [56] Y. An, H. Liu, X. Li, J. Liu, L. Chen, X. Jin, T. Chen, W. Wang, Z. Liu, M. Zhang, F.
16 Liu, Carboxymethylation modification, characterization, antioxidant activity and anti-
17 UVC ability of *Sargassum fusiforme* polysaccharide, *Carbohydr. Res.* 515 (2022).
18 <https://doi.org/10.1016/j.carres.2022.108555>.
19 [57] Y. Song, Y. Ni, X. Hu, Q. Li, Effect of phosphorylation on antioxidant activities of
20 pumpkin (*Cucurbita pepo*, Lady godiva) polysaccharide, *Int. J. Biol. Macromol.* 81
21 (2015) 41–48. <https://doi.org/10.1016/j.ijbiomac.2015.07.055>.
22 [58] J. Song, H. Chen, Y. Wei, J. Liu, Synthesis of carboxymethylated β -glucan from naked
23 barley bran and its antibacterial activity and mechanism against *Staphylococcus aureus*,
24 *Carbohydr. Polym.* 242 (2020). <https://doi.org/10.1016/j.carbpol.2020.116418>.



- 1 [59] L. Le Shao, J. Xu, M.J. Shi, X.L. Wang, Y.T. Li, L.M. Kong, R.C. Hider, T. Zhou, View Article Online
DOI: 10.1039/D5MA01478F
- 2 Preparation, antioxidant and antimicrobial evaluation of hydroxamated degraded
- 3 polysaccharides from *Enteromorpha prolifera*, *Food Chem.* 237 (2017) 481–487.
- 4 <https://doi.org/10.1016/j.foodchem.2017.05.119>.
- 5 [60] Y. Liu, Y. You, Y. Li, L. Zhang, T. Tang, X. Duan, C. Li, A. Liu, B. Hu, D. Chen,
- 6 Characterization of carboxymethylated polysaccharides from *Catathelasma*
- 7 *ventricosum* and their antioxidant and antibacterial activities, *J. Funct. Foods* 38 (2017)
- 8 355–362. <https://doi.org/10.1016/j.jff.2017.09.050>.
- 9 [61] L.Y.C. Madruga, R.M. Sabino, E.C.G. Santos, K.C. Papat, R. de C. Balaban, M.J.
- 10 Kipper, Carboxymethyl-kappa-carrageenan: A study of biocompatibility, antioxidant
- 11 and antibacterial activities, *Int. J. Biol. Macromol.* 152 (2020) 483–491.
- 12 <https://doi.org/10.1016/j.ijbiomac.2020.02.274>.
- 13 [62] R. Ruhal, R. Kataria, Biofilm patterns in gram-positive and gram-negative bacteria,
- 14 *Microbiol. Res.* 251 (2021) 126829. <https://doi.org/10.1016/j.micres.2021.126829>.
- 15 [63] S.R.M. Bushby, G.H. Hitchings, TRIMETHOPRIM, A SULPHONAMIDE
- 16 POTENTIATOR, 1968.
- 17 [64] O. Sköld, Sulfonamide resistance: Mechanisms and trends, *Drug Resistance Updates* 3
- 18 (2000) 155–160. <https://doi.org/10.1054/drup.2000.0146>.
- 19 [65] G.M. Brown, The Biosynthesis of Folic Acid II. INHIBITION BY
- 20 SULFONAMIDES*, 1962.
- 21 [66] R. Lin, J. Zhang, R. Xu, C. Yuan, L. Guo, P. Liu, Y. Fang, B. Cui, Developments in
- 22 molecular docking technologies for application of polysaccharide-based materials: A
- 23 review, *Crit. Rev. Food Sci. Nutr.* 64 (2024) 8540–8552.
- 24 <https://doi.org/10.1080/10408398.2023.2200833>.
- 25



- **The data supporting this article have been included as part of the Supplementary Information.**

